Pharmacological suppression of B7-H4 glycosylation restores antitumor immunity in immune-cold breast cancers

Xinxin Song [1*], Zhuan Zhou [1*], Hongchun Li [2,3*], Yifan Xue [4], Xinhua Lu [4], Ivet Bahar [2], Oliver Kepp [5], Mien-Chie Hung [6], Guido Kroemer [5,7] and Yong Wan [1§]

Summary of Supplementary Materials:

1. **Supplementary Figures 1-8**
2. **Supplementary Table 1**

1. Supplementary Figures 1-8

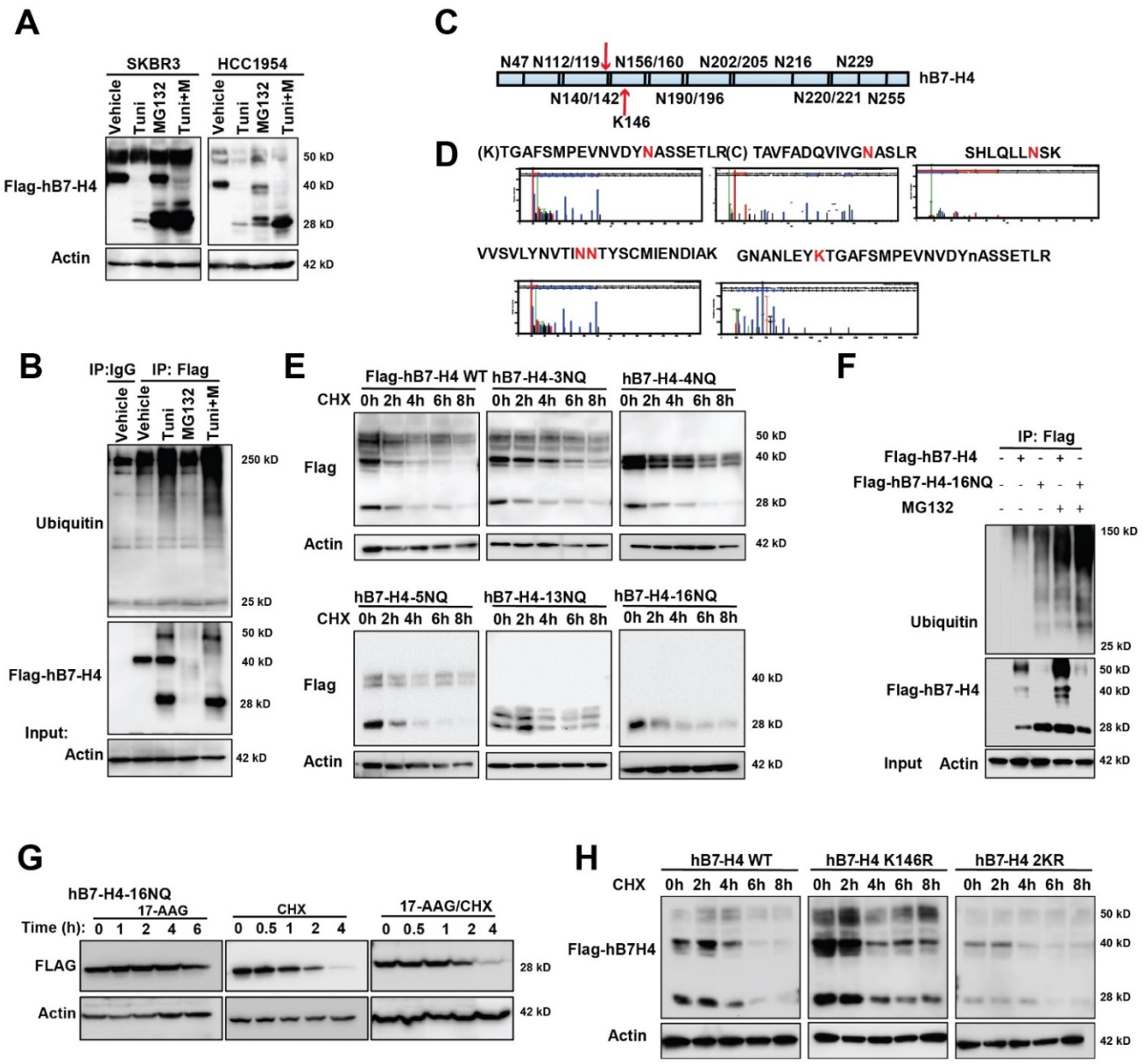

Supplementary Fig.1

Supplementary Figure 1. Identification of B7-H4 glycosylation sites and ubiquitination sites by mass spectrometry and validation by mutagenesis analysis.

(**A**) HCC1954 and SKBR3 stable expression of Flag-hB7-H4 cells were treated MG132 and/or tunicamycin followed by measuring Flag protein by western blotting. (**B**) MDA-MB-468 cells stable expression of Flag-hB7-H4 were treated MG132 and/or tunicamycin. Then Flag-hB7-H4 was immunoprecipitated by M2 beads followed by western blotting with antibody against ubiquitin. (**C**) Schematic diagram of B7-H4 showing the position of the glycosylation sites and ubiquitination sites. (**D**) Representative spectra from the mass spectrometry showing the glycosylation and ubiquitination sites. (**E**) 293T cells were transfected with Flag-hB7-H4 and mutant B7-H4 for 24 h. The protein turnover for both wildtype and mutants was measured with cycloheximide pulse-chase assay and western blotting. (**F**) Deglycosylation of B7-H4 enhances its ubiquitination. 293T cells were transfected with Flag-hB7-H4 wildtype and 16NQ mutant in the presence or absence of MG132. Flag-tagged proteins were then immunoprecipitated by anti-Flag-M2 beads followed by western blotting using antibody against ubiquitin. (**G**) 293T cells were transfected with FLAG-B7H4-16NQ and then treated with 10 μM 17-AAG (Left panel), 100 μg/ml CHX (middle panel), or pre-treated 10 μM 17-AAG for 2h and then pulse-chase with 100 μg/ml CHX (17-AAG/CHX, right panel) for indicated hours. Cell lysates were collected at indicated time point the expression of Flag-hB7-H4-16NQ was detected by anti-FLAG antibody. (**H**) 293T cells were transfected with FlagB7-H4, Flag-hB7-H4-K146R and Flag-hB7-H4-2KR for 24 h. The protein turnover for both wild-type and mutants was measured with cycloheximide pulse-chase assay and western blotting.

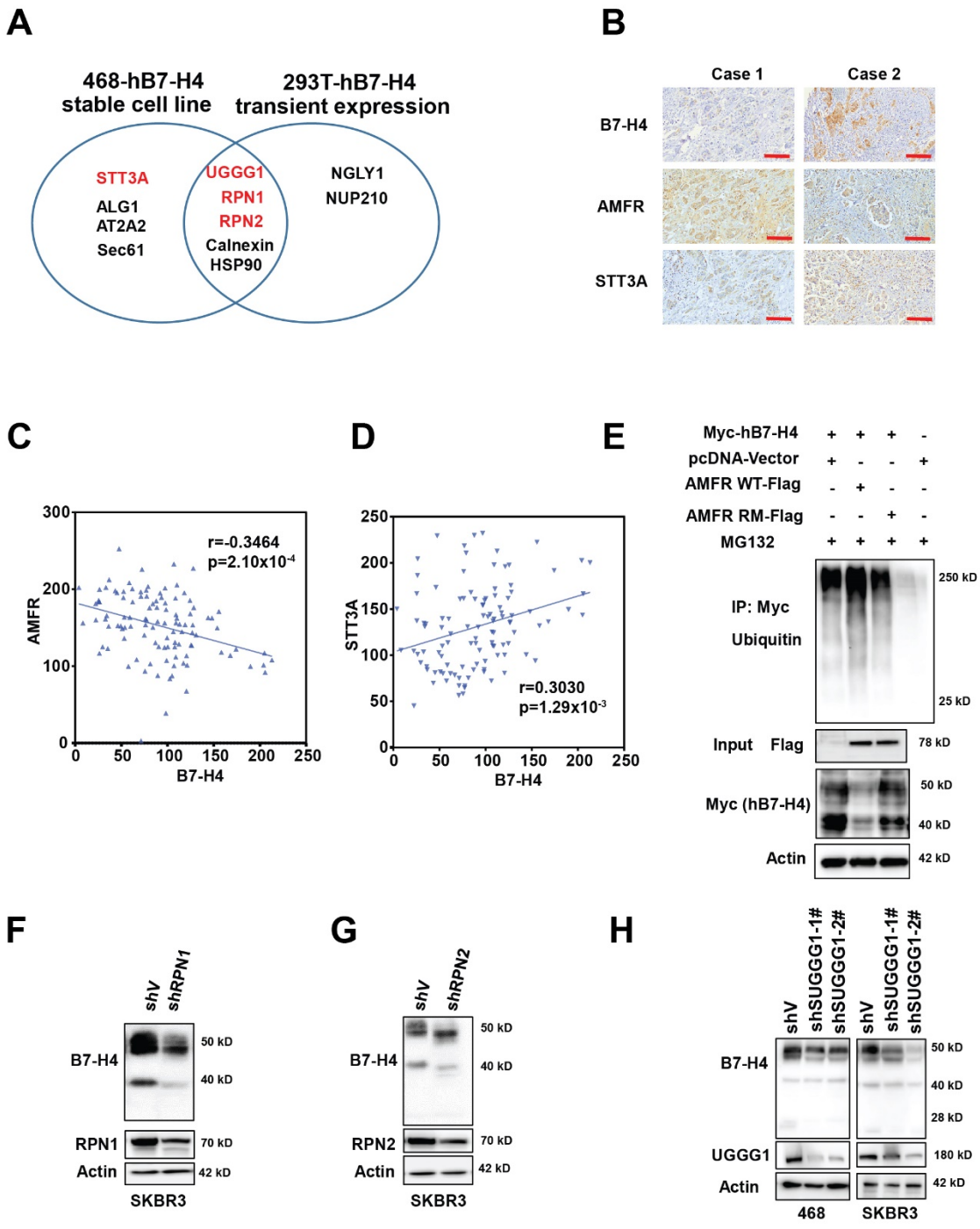

Supplementary Fig.2

Supplementary Figure 2. The identification and validation of ubiquitin E3 ligase and glycosyltransferase of B7-H4

(**A**) The Venn diagram of ER-associated B7-H4 binding partners from the mass spectrometry based on MDA-MB-468 with stable expression of Flag-hB7-H4 and 293T cells with transient expression of Flag-hB7-H4. (**B**) Representative paired immunohistochemistry staining of B7-H4, AMFR and STT3A. Scale, 200 μm. (**C-D**) Statistical analysis of immunohistochemistry staining of the tissue array shows that B7-H4 expression is negatively correlated with AMFR expression in breast cancer ($r = 0.3464$, $p = 2.1 \times 10^{-4}$) (**C**), and positively correlated with STT3A expression in breast cancer ($r = 0.3030$, $p = 1.29 \times 10^{-3}$) (**D**). (**E**) 293T cells were transfected with Myc-hB7-H4 and Flag-AMFR wildtype or RM (RING-domain mutation C356G/H361A) in the presence or absence of the proteasome inhibitor MG132. Then B7-H4-Myc was immunoprecipitated followed by western blotting with antibody against ubiquitin. (**F**-**G**) The stable knockdown RPN1 (**F**), RPN2 (**G**) and UGGG1(**H**) of MDA-MB-468 or SKBR3 cells were established. The indicated proteins were examined by western blotting.

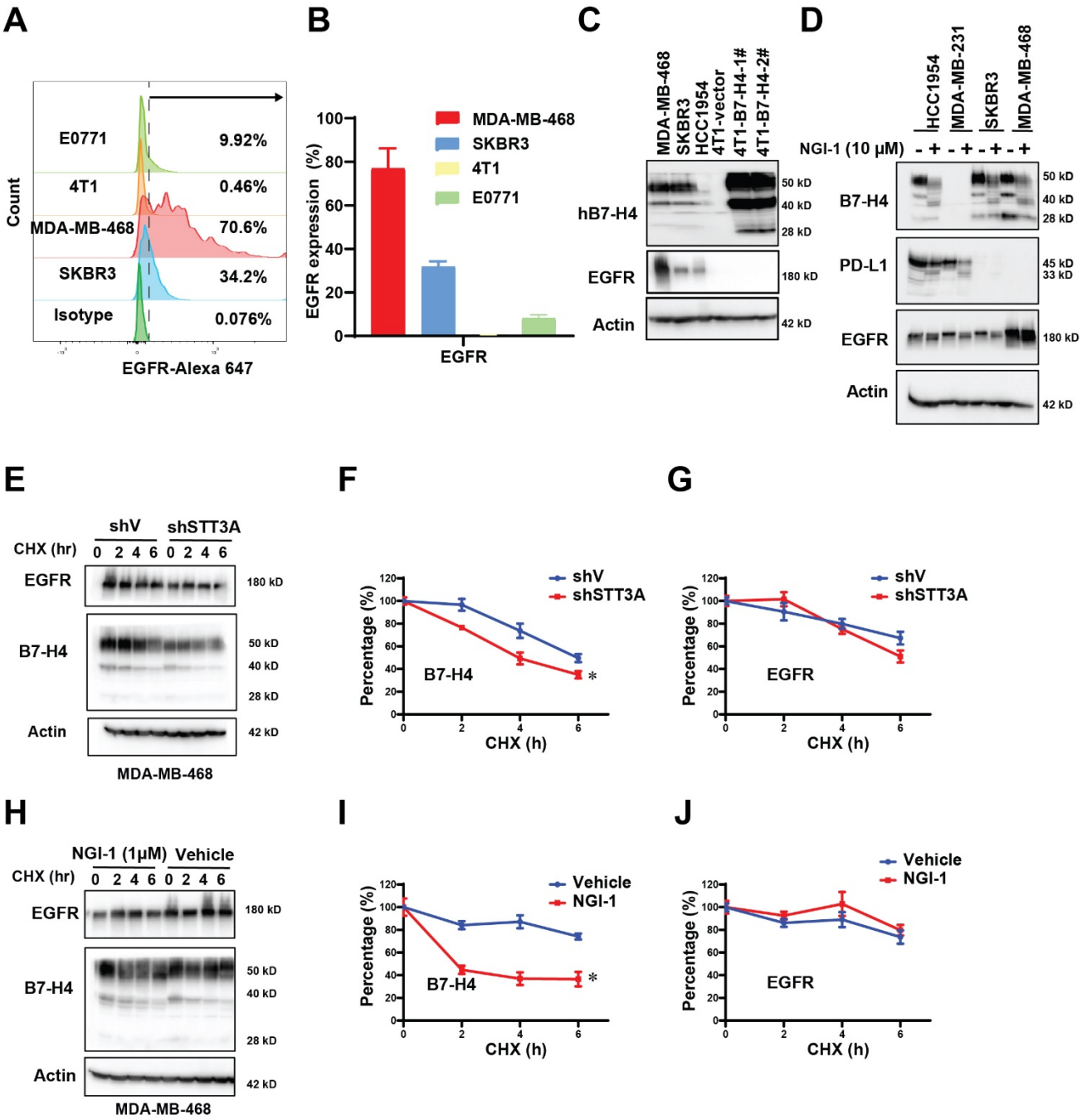

Supplementary Fig.3

Supplementary Figure 3. The comparison of the expression and the stability of EGFR with B7-H4 in breast cancer cells.

(A) The level of EGFR expression in MDA-MB-468, SKBR3, 4T1 cells and E0771 cells was examined by Flow cytometry. **(B)** Quantification of the expression of EGFR from A is shown. (C) The expression of EGFR and B7-H4 in MDA-MB-468, SKBR3, HCC1954, 4T1-vector and 4T1B7-H4 cells was examined by Flow cytometry. **(D)** HCC1954, MDA-MB-231, SKBR3, and MDAMB-468 cells were treated with NGI-1 for 24 hr followed by western blotting with B7-H4, PD-L1 and EGFR. Figure Pulse-chase analysis for MDA-MB-468 cells with STT3A knockdown or NGI-1 pre-treatment. **(E)** MDA-MB-468-shVector and -shSTT3A cells were treated with 100 μg/ml cycloheximide at the indicated time point. B7-H4 levels and EGFR were measured by western blotting. Actin was used as a loading control. **(F and G)** The quantification of B7-H4 protein and EGFR was performed using ImageLab. **(H)** MDA-MB-468 cells were pretreated with 1 μM NGI-1 for 24 hr followed by pulse-chase with cycloheximide at the indicated time point. **(I and J)** B7-H4 levels and EGFR were measured by western blotting. The quantification of B7-H4 protein and EGFR were performed using ImageLab.

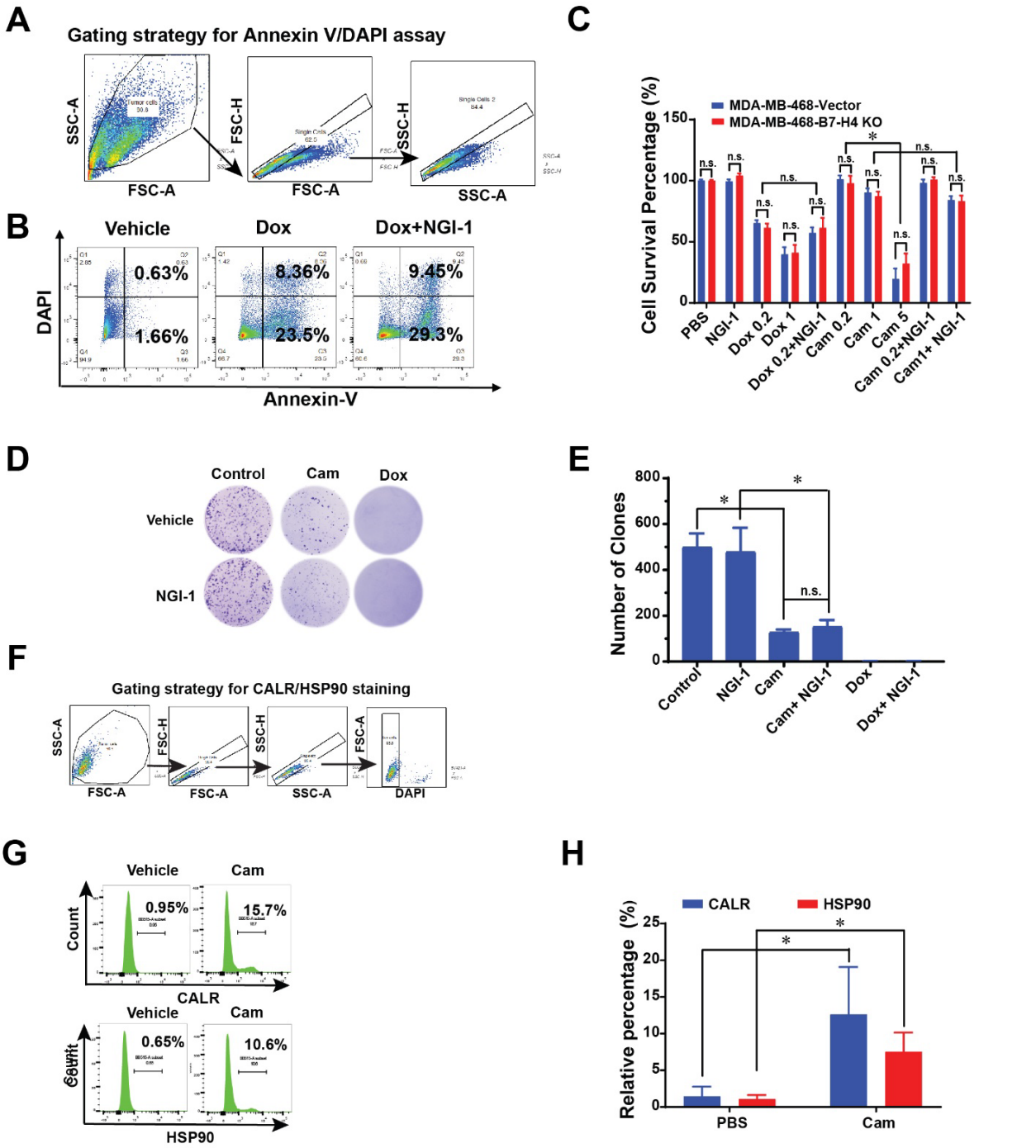

Supplementary Fig.4

Supplementary Figure 4. The effect of doxorubicin, camsirubicin and NGI-1 on cell death and DAMP molecules induction by camsirubicin in vitro.

(A) The gating strategy for Annexin V/DAPI staining. **(B)** MDA-MB-468 cells were treated with 10 μM doxorubicin in the presence or absence of 10 μM NGI-1 for 24 h. Annexin V/DAPI staining flow cytometry assay was measured. (**C**) MDA-MB-468-vector and MDA-MB-468-B7-H4 knockout cells were treated with doxorubicin (dox, 0.2-1 μM) or camsirubicin (Cam, 0.2-5 μM), or NGI-1 (10 μM) for 3 days, cell viability was measured with CCK8 assay. (**D**) MDA-MB-468 cells were treated with NGI-1 (10 μM) for 24 hr, 5 μM dox for 30 min or 5 μM cam for 30 min followed by plating 1000 cells for colony formation for 2 weeks. Representative images are shown. (**E**) Quantification of numbers of colonies from D is shown. (**F**) The gating strategy of CALR or HSP90 staining. After the debris and doublets removal, the live cells were gated based on DAPI negative cells. (**G**) MDAMB-468 cells were treated with 10 μM camsirubicin for 24 hr. Flow cytometry on the cell surface of CALR and HSP90 were performed in MDA-MB-468. (**H**) Quantification of the relative percentage of CALR and HSP90 from D in camsirubicin-treated cells.

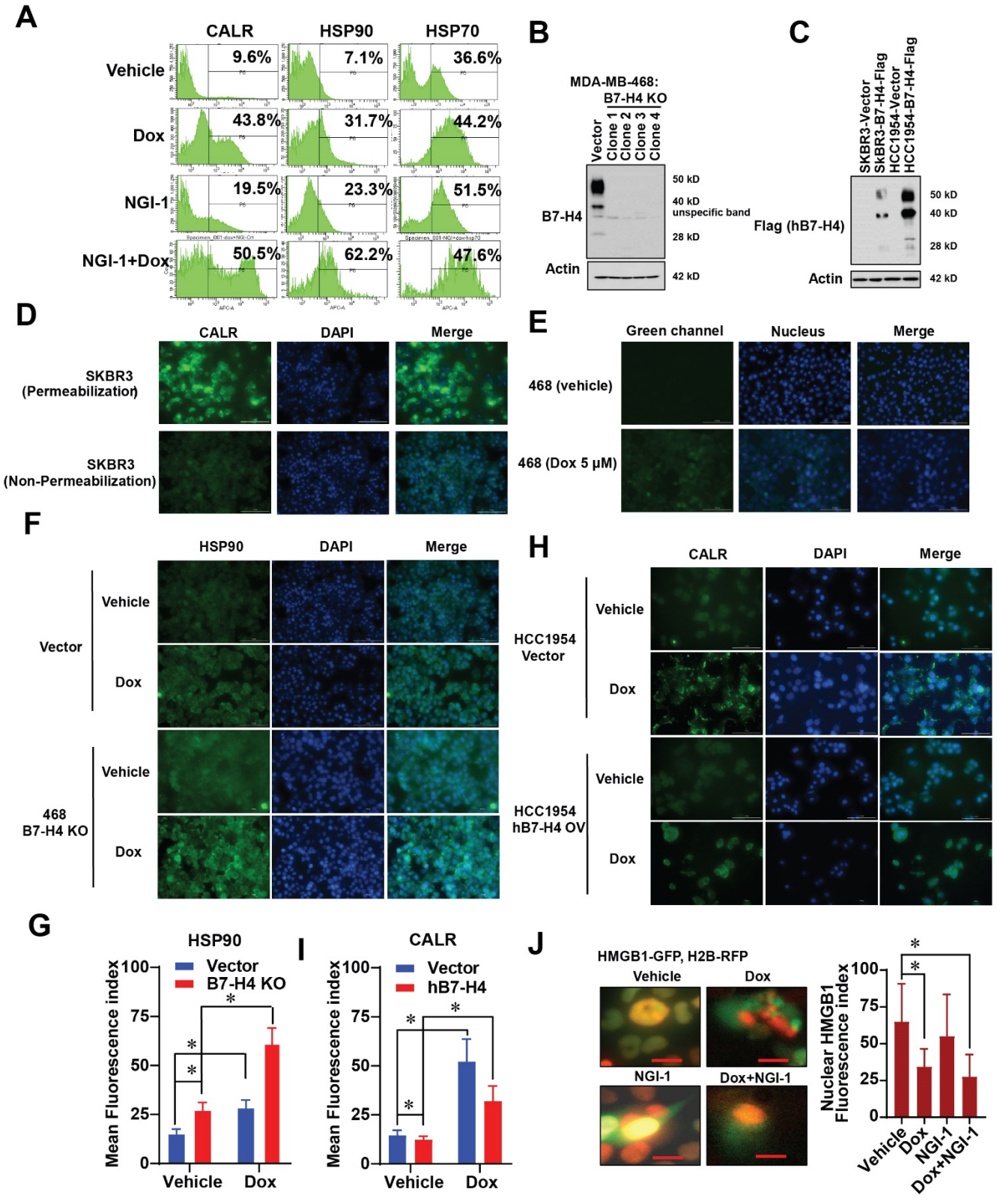

Supplementary Fig.5

Supplementary Figure 5. B7-H4 inhibits doxorubicin-induced membrane expression of damage associated molecular patterns (DAMP) molecules

(**A**) Representative flow cytometry plots showing membrane CALR, HSP70 and HSP90 of SKBR3 cells treated with doxorubicin and/or NGI-1 for 24 h. (**B**) The vector control and B7-H4 knockout clones were established in MDA-MB-468 cells. (**C**) Stable expression of Flag-hB7-H4 was established in SKBR3 and HCC1954 cells. (**D**) Immunostaining of the immunogenic cell death marker CALR of SKBR3 cells w/o permeabilization was performed. Scale = 100 μm. (**E**) The green fluorescence of MDA-MB-468 cells treated 5 μM doxorubicin at 24 hr. Scale = 100 μm. (**F**) MDAMB-468-vector and MDA-MB-468-B7-H4 knockout cells were treated with 5 μM doxorubicin for 24 h. Immunostaining of the immunogenic cell death marker HSP90 on the cell surface were performed. Scale = 100 μm. (**G**) Mean fluorescence index of HSP90 was quantified by ImageJ from F. (**H**) Membrane immunostaining of the immunogenic cell death marker CALR on HCC1954vector, and HCC1954 B7-H4 overexpressed cells were performed. Scale = 100 μm. (**I**) Mean fluorescence index of CALR was quantified by ImageJ from H. (**J**) Human osteosarcoma U2OS cell stable co-expressing HMGB1-GFP/H2B-RFP were treated with 5 μM doxorubicin and/or 10 μM NGI-1 followed by the assessment of HMGB1. Representative images are shown. Scale = 10 μm. Nuclear HMGB1 Fluorescence index was quantified by ImageJ.

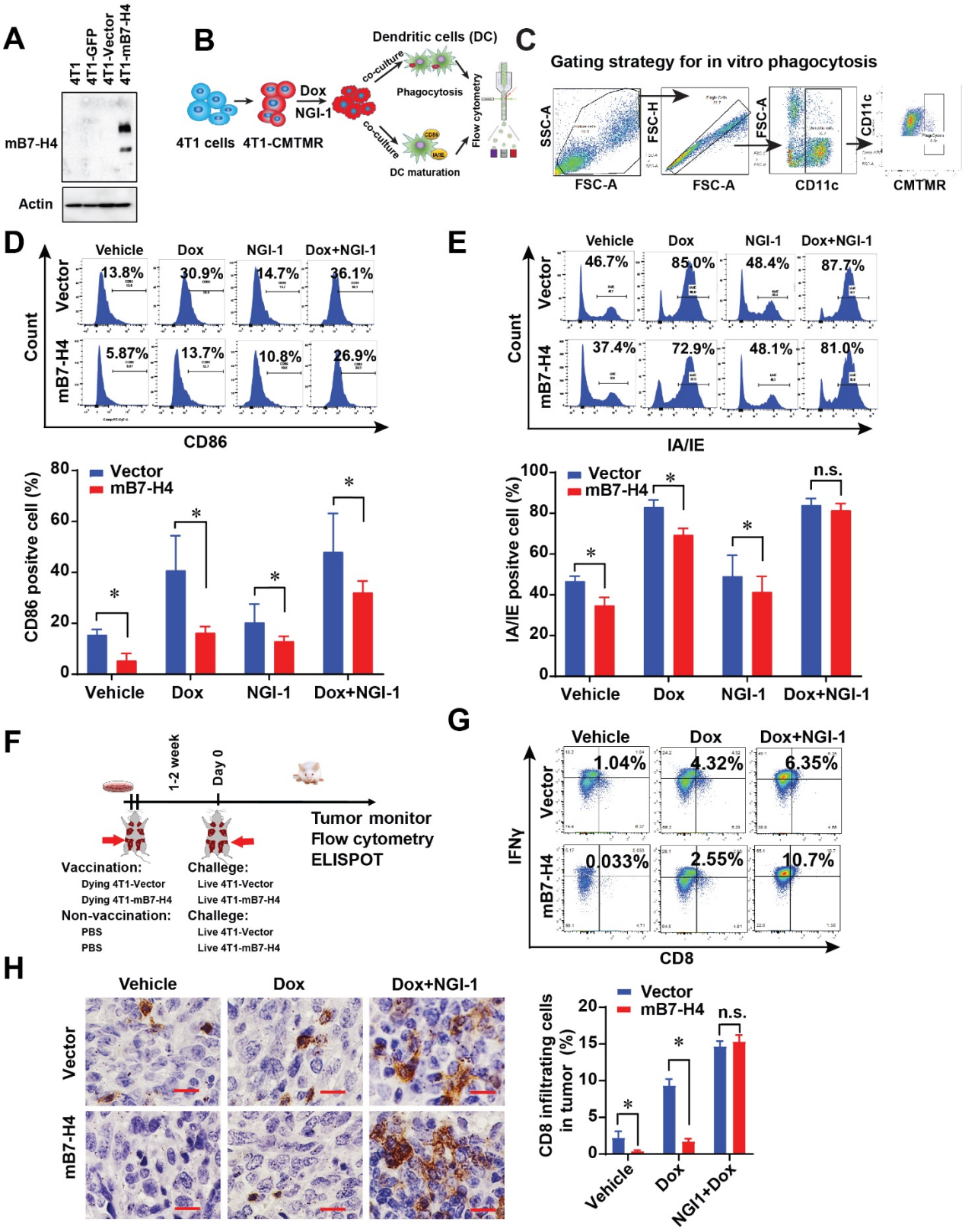

Supplementary Fig.6

Supplementary Figure 6. B7-H4 inhibits DC phagocytosis and maturation, IFNγ production and CD8 infiltration induced by doxorubicin and NGI-1-treated cancer cells.

(A) The expression of mouse B7-H4 in 4T1, 4T1-GFP, 4T1-Vector and 4T1-mB7-H4 cell lines. **(B)** Schematic diagram of in vitro phagocytosis and mouse DCs maturation assay. **(C)** Representative flow cytometry plots illustrating the typical gating strategy of in vitro phagocytosis. The DCs were gated on CD11c+. The phagocytosis is assessed as the frequency of CD11c+CMTMR+ cells events out of total CD11c+ cells. Numbers indicate frequency of events out of the previous gate. **(D-E)** DCs maturation assay. 4T1-vector and 4T1-B7-H4 cells were treated with doxorubicin (25 μM) or NGI-1 (10 μM) for 24 hours and co-cultured with the purified CD11c positive cells for 24 hours at a ratio of 1: 1, and then subjected to flow cytometry. The level of CD86 **(D)** and I-A/I-E **(E)** were measured in CD11c+ cells. Representative plots are shown. Quantification of CD86+ and I-A/I-E+ cells is shown. **(F)** Schematic diagram of the therapeutic strategy of in vivo vaccination assay. 4T1-vector or 4T1-B7-H4 cells were treated with doxorubicin and/or NGI-1 for 24 h followed by orthotopically injection into the right mammary gland of the BALB/c mice. PBS was used as the non-vaccination. One or two weeks later, all mice were rechallenged with live 4T1-vector or 4T1-B7-H4 cells in the left mammary gland. **(G)** On day 28, mouse spleens were harvested and followed by flow cytometry of staining IFNγ and CD8. The representative images are shown. **(H)** Tumor tissues were subjected to the immunohistochemistry staining with anti-CD8 antibody. The representative images are shown (scale, 20 μm). Quantification of CD8+ infiltrating cells is shown.

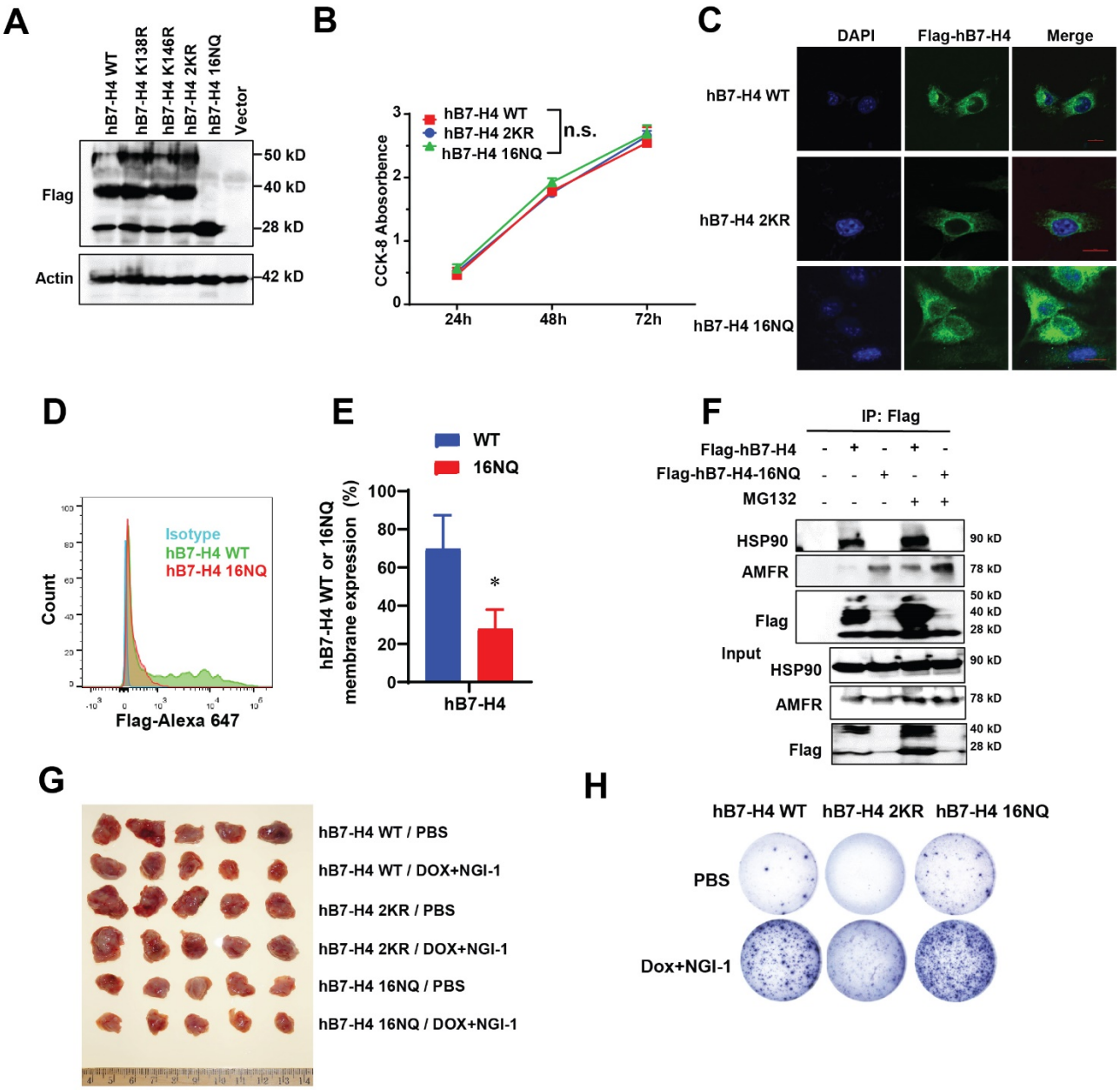

Supplementary Fig.7

Supplementary Figure 7. The comparisons of B7-H4 WT and mutants in proliferation, tumorigenesis, localization, membrane expression, and IFNγ production.

(**A**) 4T1 stably cell lines expressing Flag-tagged human B7-H4-WT, K138R, K146R, 2KR, 16NQ and vector were established, and validated by western blot using specific Flag antibody. (**B**) The proliferation assay of 4T1-B7-H4, 2KR and 16NQ cells was performed. (**C**) Immunofluorescence staining of the Flag-tagged B7-H4, 2KR and 16NQ was performed followed by confocal microscope. **(D)** The membrane expression of Flag-hB7-H4-WT and Flag-hB7-H4-16NQ. MDA-MB468 Flag-hB7-H4-WT and Flag-hB7-H4-16NQ cells were examined by flow cytometry with anti-Flag antibody followed by anti-Rabbit Alexa 647. The representative images were shown. **(E)** The quantification of the expression of B7-H4 WT or 16NQ in MDA-MB-468 Flag-hB7-H4-WT and FlagB7-H4-16NQ cells were shown. (**F**) 293T cells were transfected with Flag-hB7-H4 or Flag-hB7-H416NQ for 48 h followed by 10 μM MG132 for 8 h. Then Flag-hB7-H4 was immunoprecipitated by anti-Flag beads. The expression of HSP90, AMFR and Flag-hB7-H4 were examined by western blotting. (**G**) The representative tumor images from Fig.6F are shown. (**H**) The representative images of IFNγ ELISPOT in Fig.6G are shown.

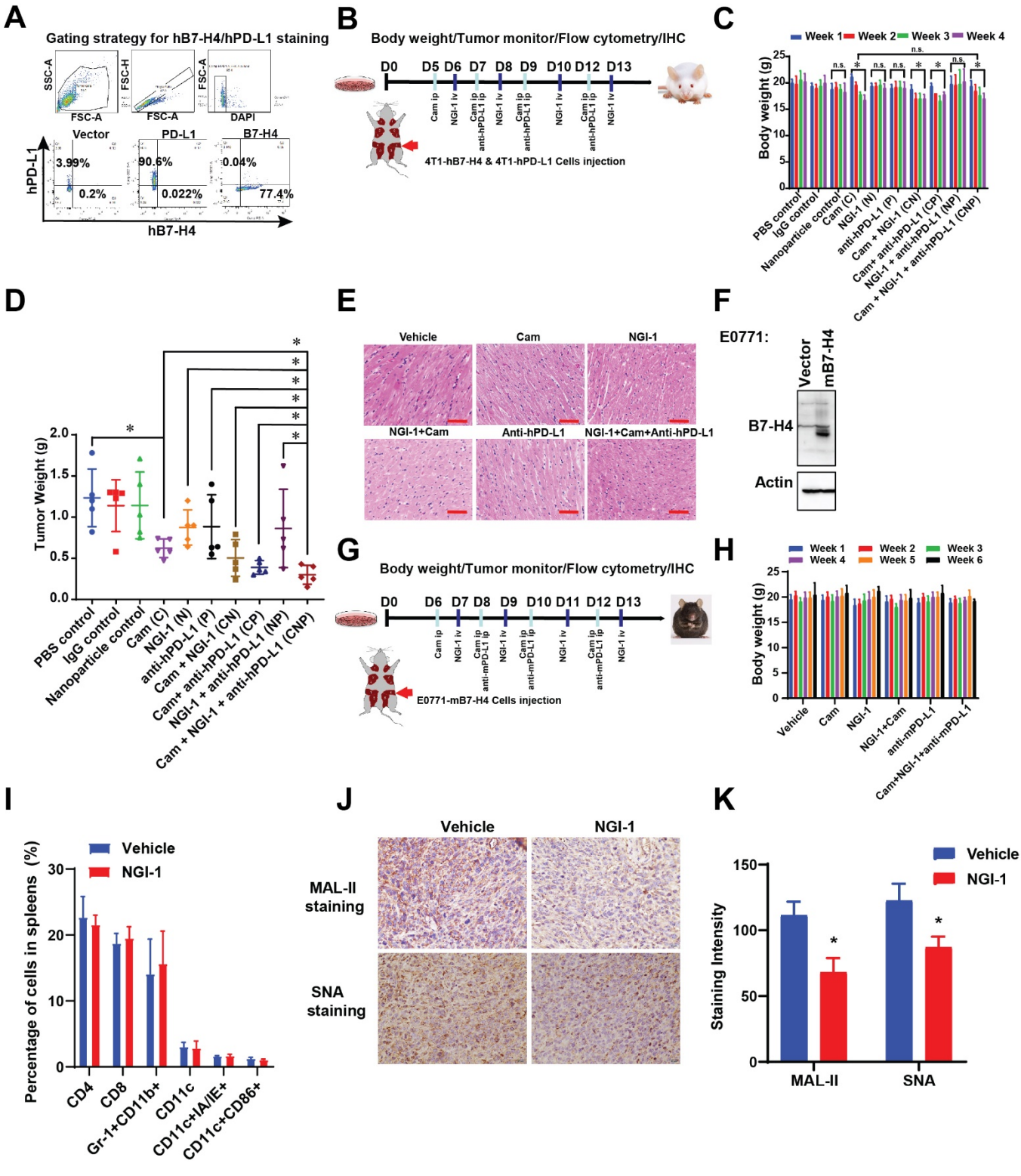

Supplementary Fig.8

Supplementary Figure 8. The therapeutic efficacy of NGI-1, camsirubicin plus PD-L1 blockade in 4T1 and E0771 breast cancer orthotopic mouse models.

(A) The gating strategy of B7-H4 or PD-L1 staining. 4T1 stably expressing hB7-H4 or hPD-L1 cells were stained with B7-H4 and PD-L1 followed by flow cytometry. (**B**) Schematic diagram of the therapeutic strategy of the combination of camsirubicin (25 mg/kg, ip.), NGI-1 (10 mg/kg, iv.) and PD-L1 antibody durvalumab (5 mg/kg, ip.) in Balb/C mice. (**C**) Body weight was monitored for 4 weeks after the injections of 4T1-B7-H4 and 4T1-PD-L1 cells. (**D**) On day 28, tumor weight was measured. (**E**) On day 28, mouse hearts from the indicated groups were subjected to H&E staining. The representative images are shown. Scale bar, 200 μm. **(F)** The expression of mouse B7-H4 in E0771 and E0771-mB7-H4 cell lines. (**G**) Schematic diagram of the therapeutic strategy of the combination of camsirubicin (5 mg/kg, ip.) NGI-1 (10 mg/kg, iv.) and anti-mPD-L1 antibody (5 mg/kg, ip.) in C57BL/6 mice. (**H**) Body weight was monitored for 6 weeks after the injections of E0771-mB7-H4 cells. **(I)** Spleen cells from C57BL/6 mice were treated with 10 μM NGI-1 for 24 hr followed by flow cytometry. The percentage of T cells, immature myeloid cells and dendritic cells were examined. n=3 mice per group. **(J)** NGI-1 inhibits both α-2,3 and α-2,6 linkage sialylation. SNA and MAL-II lectin staining were performed on the tumor tissues of the control group and NGI1 group of Balb/C mice on day 28. **(K)** The quantification of the staining intensity of MAL-II and SNA were shown.

2. Supplementary Table 1

Summary for B7-H4 expression pattern in breast cancer lines. The expression level of B7-H4 and PD-L1 in the 45 breast and 4 ovarian cancer cells were quantified by Image Lab.

Cell lines	ER	PR	HER2	B7-H4	PD-L1
SK-BR-3	N	N	Y	10.49	0
HCC202	N	N	Y	9.89	0
MCF-7	Y	Y	N	9.04	0
BT474	Y	Y	Y	5.514	0
CAMA-1	Y	N	N	4.885	0
HCC2157	N	N	N	4.87	0
HCC1569	N	N	Y	4.803	0
ZR-75-30	Y	N	Y	4.776	0
ZR-75-1	Y	Y	N	4.508	0
Au-565	N	N	Y	4.349	0
MDA-MB-415	Y	N	N	4.288	0
HCC1428	Y	Y	N	3.953	0
MDA-MB-468	N	N	N	3.232	0
HCC1187	N	N	N	2.574	0.77
HCC1954	N	N	Y	2.549	2.92
HCC1599	N	N	N	2.545	0
MDA-MB-361	Y	N	Y	2.439	0
HCC1419	Y	N	Y	2.256	0
MDA-MB-175VII	Y	N	N	2.09	0
HCC70	N	N	N	1.948	2.81
MDA-KB2	N	N	N	1.934	0

HCC1937	**N**	**N**	**N**	**1**	**1**
BT483	**Y**	**Y**	**N**	**1**	**0**
HCC2218	**N**	**N**	**Y**	**0.917**	**0**
UACC812	**Y**	**Y**	**Y**	**0.702**	**0.25**
T47D	**Y**	**Y**	**N**	**0.569**	**0.37**
HCC1500	**Y**	**N**	**N**	**0.498**	**0.2**
MDA-MB-453	**N**	**N**	**N**	**0.342**	**0**
HCC38	**N**	**N**	**N**	**0.274**	**3.31**
Hs578Bst	**N**	**N**	**N**	**0.248**	**4.28**
PA-1	**Y**	**N**	**N**	**0.114**	**0**
MDA-MB-231	**N**	**N**	**N**	**0**	**3.12**
HCC1806	**N**	**N**	**N**	**0**	**1**
MDA-MB-436	**N**	**N**	**N**	**0**	**1.14**
BT-549	**N**	**N**	**N**	**0**	**2.52**
Du4475	**N**	**N**	**N**	**0**	**0**
BT-20	**N**	**N**	**N**	**0**	**3.34**
MDA-MB-157	**N**	**N**	**N**	**0**	**0**
Hs578T	**N**	**N**	**N**	**0**	**1.88**
HCC1395	**N**	**N**	**N**	**0**	**0.2**
CaOV-3	**Y**	**N**	**N**	**0**	**2.23**
SK-OV-3	**N**	**Y**	**Y**	**0**	**1.2**
MDAMB134-VI	**Y**	**N**	**Y**	**0**	**0.58**
UACC893	**N**	**N**	**Y**	**0**	**0.18**
SW626	**N**	**N**	**Y**	**0**	**3.31**
MCF-10F	**N**	**N**	**N**	**0**	**0.51**

MCF-12A	**Y**	**N**	**N**	**0**	**0.22**
184-B5	**N**	**N**	**N**	**0**	**0.3**
MCF-10A	**N**	**N**	**N**	**0**	**0.02**

N, Negative; Y, Positive; ER, estrogen receptor; PR, Progesterone receptor; HER2, human epidermal growth factor receptor 2.